The Journal of Neuroscience, October 1993, 13(10): 4511–4524

Structural and Functional Specialization of Aδ and C Fiber Free Nerve Endings Innervating Rabbit Corneal Epithelium

M. Bruce MacIver and Darrell L. Tanelian[a]

Pain Research Laboratory, Department of Anesthesia, Stanford University School of Medicine, Stanford, California 94305-5117

An *in vitro* preparation of rabbit cornea was used to compare anatomical specialization and electrophysiological responses of Aδ and C fiber sensory afferents which terminate as free nerve endings. Living nerve endings were visualized using epifluorescence microscopy and the vital dye 4-di$_2$-ASP, and response properties were determined using microstimulation and recording of fiber discharge activity. Fiber type was determined based on conduction velocity measurement and preferred stimulus energy (modality) of each fiber. Four modality-specific fiber populations were identified: (1) slowly adapting C fiber cold receptors (conduction velocity of 0.25–1.6 m/sec), (2) C fiber chemosensitive units with mixed phasic and tonic activity (1.1–1.8 m/sec), (3) rapidly adapting mechanosensitive Aδ fibers (1.5–2.8 m/sec), and (4) high-threshold mechano/heat (>350 dyne or >40°C) phasic Aδ afferents (3.5–4.4 m/sec). In addition to these physiological differences, anatomical specialization was also noted. Aδ fiber nerve endings were distinguished from those of C fibers by thin, elongated sensory endings that ran parallel to the corneal surface; C fiber endings formed short, branching clusters that ran mostly perpendicular to the surface. The elongated structure of Aδ nerve endings was associated with directional selectivity for mechanical stimuli. These results substantiate previous suggestions that free nerve endings can exhibit both structural and functional specialization.

[Key words: pain fiber, nociceptor, mechanoreceptor, thermoreceptor, chemoreceptor, sensory transduction, somatosensory, epifluorescence, 4-di$_2$-ASP]

Studies of Aδ and C fiber free nerve endings have been limited by an inability to compare simultaneously their structural and functional properties. This limitation is due to an intimate association between free nerve endings and surrounding tissue elements; it has not been possible to isolate these nerve endings without destroying them, and microscopic studies of living nerve endings *in situ* have been hindered by a lack of tissue transparency. Thus, it has not been possible to test directly whether free nerve ending specializations, observed in ultrastructural studies, are associated with functionally distinct subpopulations of afferent fibers (Hensel et al., 1974; Kruger et al., 1985; Heppelmann et al., 1990). Conversely, physiological studies have shown functional differences exist among subgroups of Aδ and C fibers (Campbell et al., 1979; Belmonte et al., 1991), but correlations to differences in nerve ending anatomy are lacking.

Corneal epithelial tissue is transparent and innervated exclusively by Aδ and C fibers which terminate as free nerve endings (Zander and Weddell, 1951; Rozsa and Beuerman, 1982; Harris and Purves, 1989; Tanelian and MacIver, 1990). Thermal, chemical, or mechanical stimulation of the cornea produces sensations of irritation and pain in humans (Kenshalo, 1960; Schirmer, 1963; Beuerman et al., 1977; Beuerman and Tanelian, 1979) and defensive reflexes in animals (Janesco et al., 1961). This is consistent with Aδ and C fiber nerve activity being associated with nociception (Ochoa and Torebjork, 1989; Ness and Gebhart, 1990). Since corneal tissue is avascular, neural responses secondary to changes in vascular integrity are eliminated, and the cornea consists of a simple connective tissue matrix between an unkeratinized epithelium and endothelium, reducing complex tissue interactions. Free nerve endings terminate within 5 μm of the unkeratinized epithelial surface of the cornea, providing unparalleled access for experimental stimulation. In addition, living nerve endings and fibers in the epithelium can be visualized and electrophysiologically characterized (Harris and Purves, 1989; Tanelian and MacIver, 1990), allowing detailed structure–function relationships to be explored.

Several electrophysiological investigations of corneal nerves have been undertaken (Tower, 1940; Lele and Weddell, 1959; Dawson, 1962; Mark and Maurice, 1977; Belmonte and Giraldez, 1981; Tanelian and Beuerman, 1984; Jarvis et al., 1990; MacIver and Tanelian, 1990; Tanelian and MacIver, 1990; Belmonte et al., 1991), but none have characterized response thresholds and fiber types for all stimuli known to elicit corneal pain. The electrophysiological data, however, have provided support for functional specialization among the population(s) of corneal Aδ and C fibers (see Discussion). In the present study we investigated whether structural and functional specialization exists for free nerve endings innervating rabbit corneal epithelium.

Materials and Methods

Tissue isolation. The experimental protocol was approved by the Institutional Animal Care Review Committee at Stanford University and

Received Jan. 8, 1993; revised Apr. 27, 1993; accepted May 3, 1993.

We thank Drs. Daniel V. Madison and Istvan Mody for comments on an early version of the manuscript, and Dr. Carla J. Shatz for providing advice and an epifluorescent microscope during the early stages of this study. Mr. Francis Lundy of Technical Instruments Co. provided invaluable support with custom optics and micromanipulators. This work was supported by a grant from the National Institute of Health (RO1 NS28646-01).

[a]Correspondence should be addressed to Darrell L. Tanelian at his present address: Department of Anesthesiology and Pain Management, University of Texas Southwestern Medical Center, Dallas, Texas 75235-9068.

Copyright © 1993 Society for Neuroscience 0270-6474/93/134511-14$05.00/0

care was taken at all stages of handling to minimize stress and discomfort for the animals. Thirty-seven albino rabbits (New Zealand White) weighing 2.5–3.0 kg were obtained from Nittabell Inc. and housed on a 12:12 hr light/dark cycle. Animals were anesthetized by intramuscular injection of ketamine (40 mg/kg) and xylazine (5 mg/kg, i.p.), and then killed with Beuthanasia (1.0 ml, i.v.).

The cornea, together with 3–5 mm of sclera, was rapidly excised and placed in cooled (5°C) and oxygenated artificial aqueous humor solution (AQH; see Materials, below). Extraneous conjunctivae and ocular musculature, together with the lens, iris, and retina, were removed taking care not to damage either the epithelium or endothelium on the inside of the cornea. This isolation procedure was carried out in cold AQH and required less than 5 min.

Tissue chamber. The tissue chamber allowed continuous perfusion with AQH behind the cornea at a constant temperature (35°C) and pressure (18 mm Hg) to reproduce *in vivo* conditions. The cornea was placed over a Plexiglas ring and a watertight seal was formed by securing the sclera with a compression suture (Fig. 1*A*). An outer chamber was filled with normal saline warmed by a circulating water bath and heat exchanger, and an aerating stone placed in the saline provided a constant stream of prewarmed and humidified carbogen (O_2:CO_2, 95:5%; 3 liters/min) to the corneal surface. This moistened carbogen atmosphere prevented drying of the corneal surface. A second heat exchanger in the outer bath warmed the AQH solution before it entered the inner chamber. Probes were placed inside the chamber to monitor pressure and temperature. Fiber-optic light guides provided illumination of corneal tissue from above and below to view corneal nerve bundles with a variable magnification stereo microscope (Wild M3Z).

Staining and photography. Corneal nerve endings were stained with 4-di$_2$-ASP [Molecular Probes, Inc.; 4-(4-diethylaminostyryl)-*N*-methylpyridinium iodide] at a 10 μM concentration in the AQH perfusate (Harris and Purves, 1989; Tanelian and MacIver, 1990; LaMantia et al., 1992). Optimal visualization required 1.0–1.5 hr of staining time at 35°C, and more than 2 hr at room temperature. Nerve endings were photographed with Kodak Plus-X 125 using a Leitz epifluorescence microscope with both air and water emersion objectives (Leitz 20×, 25×, 32×, and Nikon 40×), and Leitz excitation/emission (490/610 nm) filters. Illumination was provided by an Osram 100 W mercury light source and Leitz model 1230 power source. Optics, micromanipulators, and a custom optics carrier, which allowed microscope placement and precision movement over the cornea, were supplied by Technical Instruments Co. (San Francisco, CA).

Electrophysiology. Extracellular action potential recordings were obtained using suction electrodes [100–250 μm, 10–50 KΩ; World Precision Instruments Inc. (WPI); thin wall 1.0 mm o.d. fiberfill glass, filled with AQH] placed on small corneal nerve bundles at the cornea–sclera border (limbus; see Fig. 1*B*). Electrodes were DC coupled to the active head stage of a cathode follower (WPI model DAM 5A) and amplified (1000×). Signals were further amplified (20×), filtered (10 Hz to 30 kHz, bandpass), and conditioned (DC offset or AC coupled) prior to being digitally stored (50 kHz) for computer analysis (Strathclyde Electrophysiological Software and Brain Wave Systems Corp.). Continuous recordings of discharge activity were analyzed for changes in spike frequency. Mechanically or electrically activated fibers were analyzed for action potential amplitude, spike dV/dt, and latency from stimulus to peak voltage.

Electrodes and stimulus probes were carried on precision micromanipulators (Leitz and Narishige) and placed under visual guidance onto the corneal surface. Vibration was minimized using an air-damped isolation table (MICRO-g). AQH solution was delivered to the inner chamber via Teflon tubing and constant pressure and flow rate were maintained.

Stimulation. Mechanical stimuli were produced using fine calibrated nylon filaments coupled to an electromagnetic transducer driven by square wave pulses (2.0–5.0 msec) at a rate of 0.1 Hz. The filaments were microbalance calibrated (stimulus voltage of 1.0 V produced 62 mg; 1.0 mg/mm^2 = 0.98 dyne/mm^2). In most experiments, receptive fields for mechanosensitive fibers were initially mapped using calibrated von Frey filaments.

Electrical stimuli were produced using bipolar tungsten microelectrodes (9–12 MΩ) and stimulus intensities of 1.0–10 V (constant current isolation). Polarity and pulse duration (0.05–0.25 msec) were varied, together with tip placement (in 10 μm increments) to minimize the current intensity needed to stimulate isolated single-fiber responses. Stimulation of individual free nerve endings was evident when only a single action potential was elicited by low stimulus currents, and small changes in location (<50 μm) of the stimulating electrode abolished responses. Excitability maps were generated by applying a train of 10–100 stimuli (0.5 Hz) at each point, forming a 20 × 20 grid in a 2 mm^2 area surrounding a previously identified receptive field of a fiber. Stimulus intensity was set at 1.5 times threshold to ensure activation only when the stimulating electrode was in the immediate vicinity of nerve endings. Data were then plotted as the response:stimulus ratio for each point, with an interpolation factor of three to generate a 60 × 60 grid map (e.g., Fig. 2*A,B*; see also Fig. 7*C*). Conduction velocities were measured by applying an electrical stimulus to the terminal field of a fiber and measuring the distance between the stimulating and recording electrodes with a fine suture thread to follow the branching and curved trajectory of each nerve fiber. This method would be expected to underestimate conduction velocities of Aδ fibers since they lose myelination as they terminate within the cornea (Belmonte and Giraldez, 1981; Beuerman et al., 1983).

Temperature of the corneal surface was changed by applying 1.0 ml of preheated or cooled AQH solution (15–50°C) to the epithelial surface from a temperature exchange system coupled to a Narishige microinjector. Adaptation was tested by applying successive thermal stimuli at short intervals (1–2 sec). Rapid heating of sensory terminals was accomplished using a pulsed CO_2 laser (Coherent Medical Inc.) with a small spot size (2 mm^2) focused on the corneal surface. Intensity and duration of laser irradiation were varied to produce thermal effects without damaging the epithelium. Stimulus parameters and temperature determination were based on thermodynamic modeling of corneal epithelial absorption of laser energy (Jarvis et al., 1990). Chemical stimulation was provided by dissolving the agents in AQH solution and applying these solutions at 37°C to the corneal epithelium via a Narishige microinjector system (1.0 ml). This volume was sufficient to cover the entire corneal surface and the force component of the fluid was less than the threshold for activation of mechanosensitive fibers.

Materials. The AQH solution contained the following (mM): Na, 145; K, 4.5; Ca, 1.5; Mg, 0.6; Cl, 126.3; SO_4, 0.6; HPO_4, 0.6; HCO_3, 25; glucose, 10. All chemicals were reagent grade or better and were obtained from J. T. Baker Chemical Co. as the hydrated salt. Acetylcholine, carbachol, nicotine, bethanecol, *d*-tubocurare, atropine, glutamate, *N*-methyl-D-aspartate (NMDA), 2-amino-5-phosphonovalerate (APV), bradykinin, and prostaglandin E_1 were obtained from Sigma Chemical Corp. α- and κ-bungarotoxin were obtained from Calbiochem. Ketamine HCl (Ketaset) was obtained from Aveco Co., Inc.; and MK 801, from Merck Sharp and Dohme, Inc. Water for solutions was HPLC and spectrophotometry grade and obtained from EM Science. AQH solutions were chilled to 5°C and saturated with carbogen prior to use. After warming to 35°C, solutions had a pH of 7.2–7.4.

Results

Morphology of Aδ and C fiber nerve endings

By simultaneously observing and stimulating nerve endings while recording action potential discharges from their corresponding axons, it was possible to distinguish differences in nerve ending morphology between Aδ and C fibers. Aδ fibers exhibited conduction velocities >1.5 m/sec and action potential amplitudes of >200 μV, following electrical stimulation of the corneal surface (Fig. 1). Aδ nerve endings appeared to be made up of several (two to eight) thin, elongated strands emerging from a common point at the end of a fiber as it entered the epithelium, or emerging en passant from leashes in the basal epithelium. The strands ran parallel to each other, and to the corneal surface, at a depth of 10–40 μm and for distances of 200 μm to 2.5 mm. Each strand appeared to weave between epithelial cells but would converge periodically to rejoin the other strands making up each nerve ending (Fig. 1*B*). Aδ nerve ending strands were readily distinguished from bundles of axons that formed corneal leashes as they emerged from the subepithelial plexus. Leash axons were localized to the basal epithelial cell layer and gave rise to both Aδ and C fiber endings that terminated in the superficial epithelial layers.

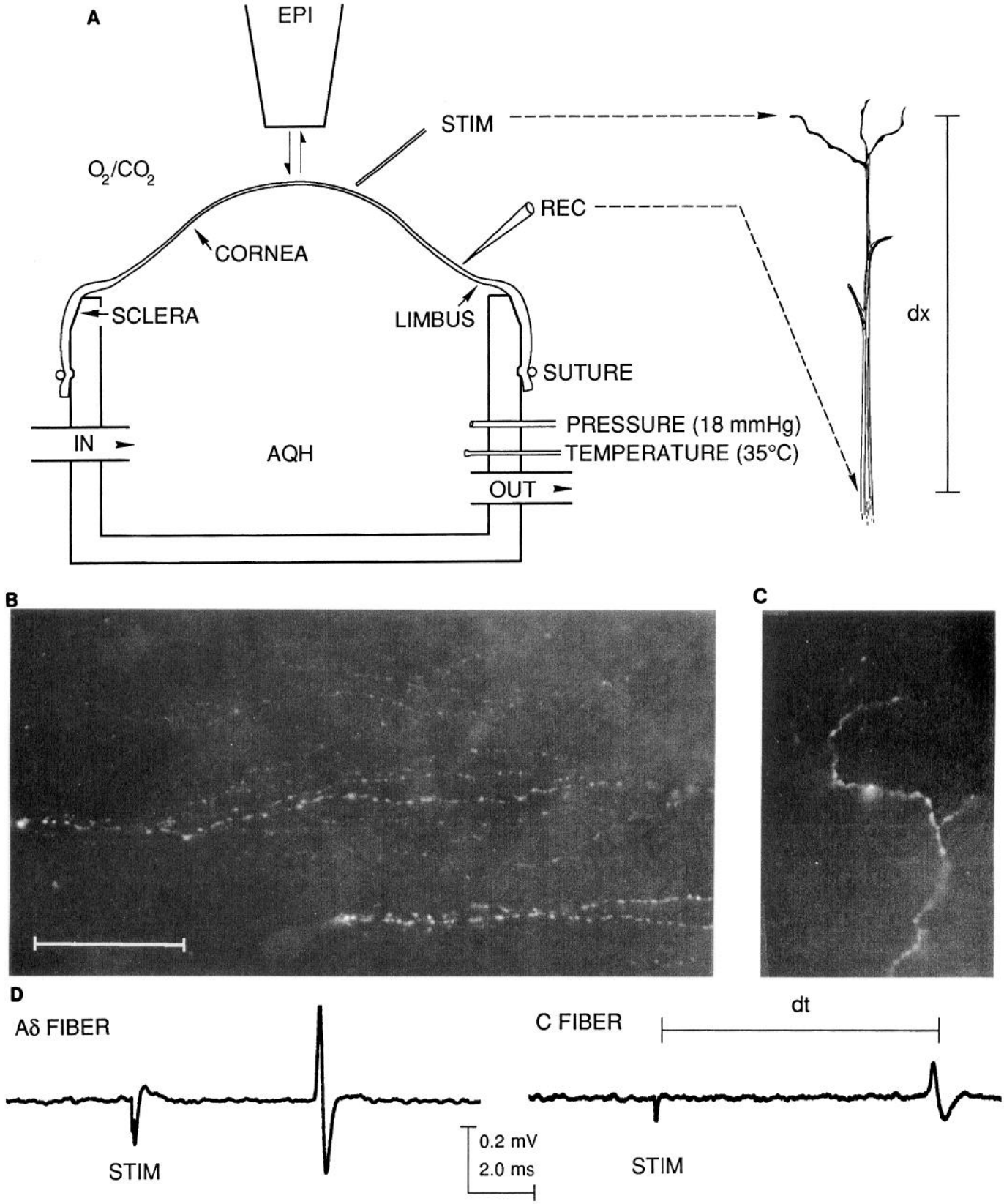

Figure 1. *A* is a diagram of the tissue chamber showing the relative positions of stimulus probe (*STIM*), extracellular recording electrode (*REC*), pressure monitor, temperature monitor, and inlet and outlet (*IN/OUT*) for perfusion of AQH. The epithelial surface was kept moist by humidified and warmed carbogen (O_2/CO_2) gas. Sensory nerve endings and fibers were visualized with epifluorescent (*EPI*) microscopy, following staining with the vital dye 4-di$_2$-ASP. *B* is an epifluorescence micrograph of an identified Aδ fiber nerve ending: note the thin, elongated fibers that run parallel to each other and to the corneal surface at a depth of 20–40 μm. *C* is an epifluorescence micrograph of an identified C fiber nerve ending showing the extensive branching pattern that approaches to within 5 μm of the corneal surface. Scale bar (*B*), 10 μm for *B* and *C*. Fibers were identified on the basis of conduction velocity (*dx/dt*), with Aδ fibers usually conducting at greater than 2.0 m/sec and C fibers at 0.25–1.5 m/sec. *D* shows single isolated unit recordings from fibers whose nerve endings are shown in *B* and *C*, following electrical stimulation (*STIM*) of the nerve endings. In addition to faster conduction velocities, Aδ fibers usually had larger action potential amplitudes compared with C fibers.

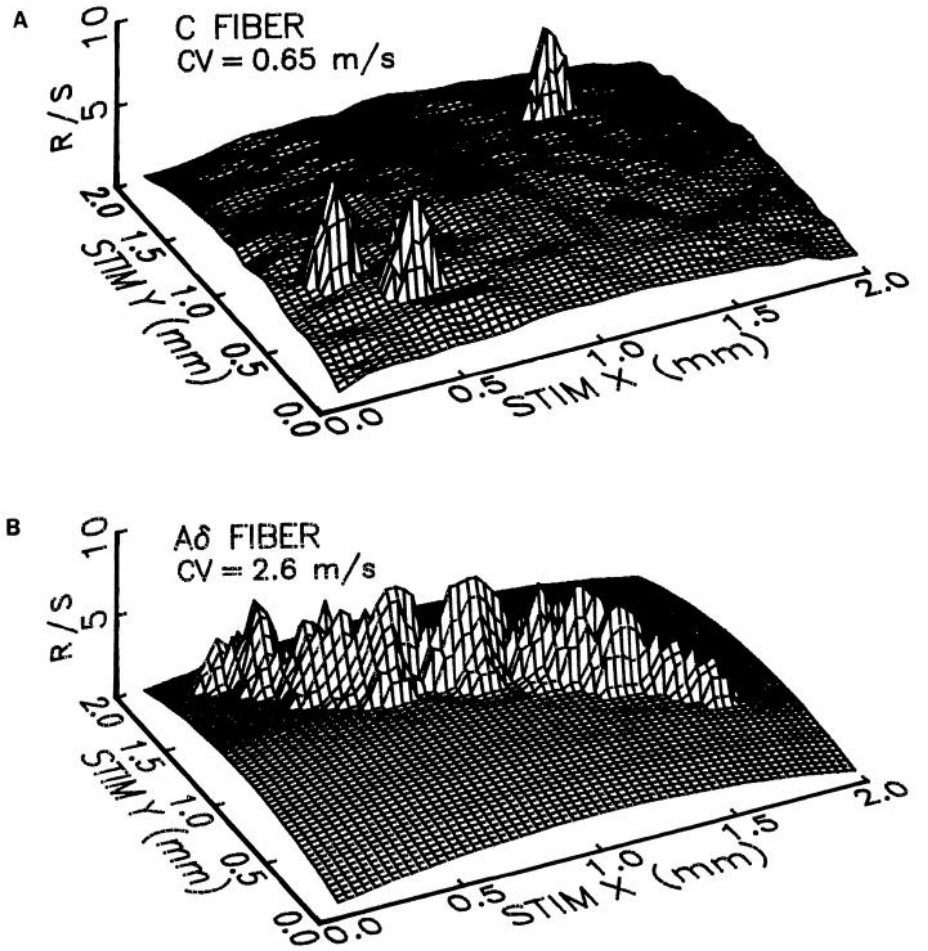

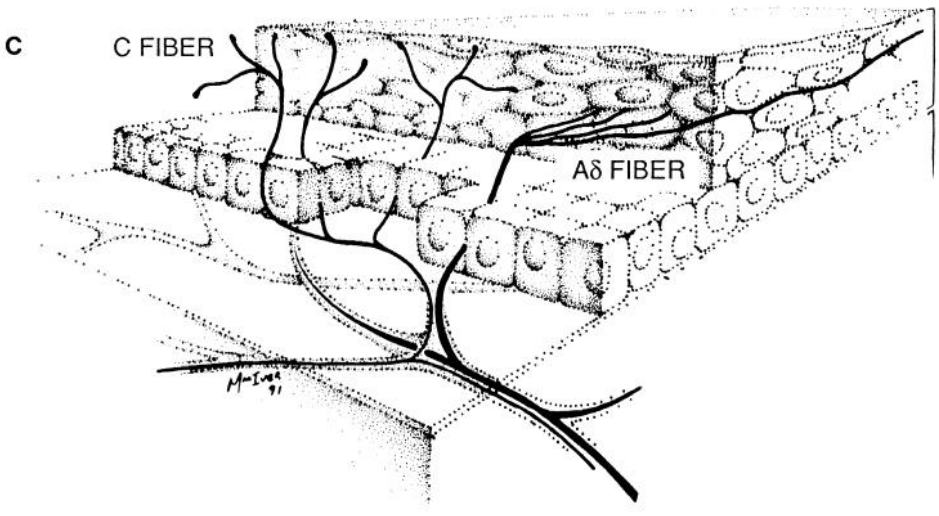

Figure 2. Morphologically distinct ending patterns for Aδ and C fibers were apparent from both epifluorescence microscopy and excitability maps that plot discharge probability in response to a constant threshold stimulus. Excitability maps (*A* and *B*) for identified C fibers showed narrow peaks of activity that were invariably situated above clusters of branched endings near the corneal surface. A given C fiber had one to seven response peaks within a 2 mm^2 test area, with each peak located above a cluster of endings. Aδ fibers exhibited elongated linear profiles that closely paralleled the thin, elongated endings observed with epifluorescence microscopy. The excitability maps shown in *A* and *B* were from the Aδ and C fiber in Figure 1. The diagram shown in *C* indicates how Aδ and C fiber endings terminate among corneal epithelial cells.

C fibers also responded to electrical stimulation of the corneal surface and had conduction velocities of <2.0 m/sec with action potential amplitudes between 25 and 300 μV. C fiber nerve endings formed short branching clusters that emerged from single fibers as they arose from the subepithelial plexus and/or basal leash axon bundles. Terminal endings generally traveled in a vertical manner, but twisted, turned, and branched frequently as they approached to within a few micrometers of the

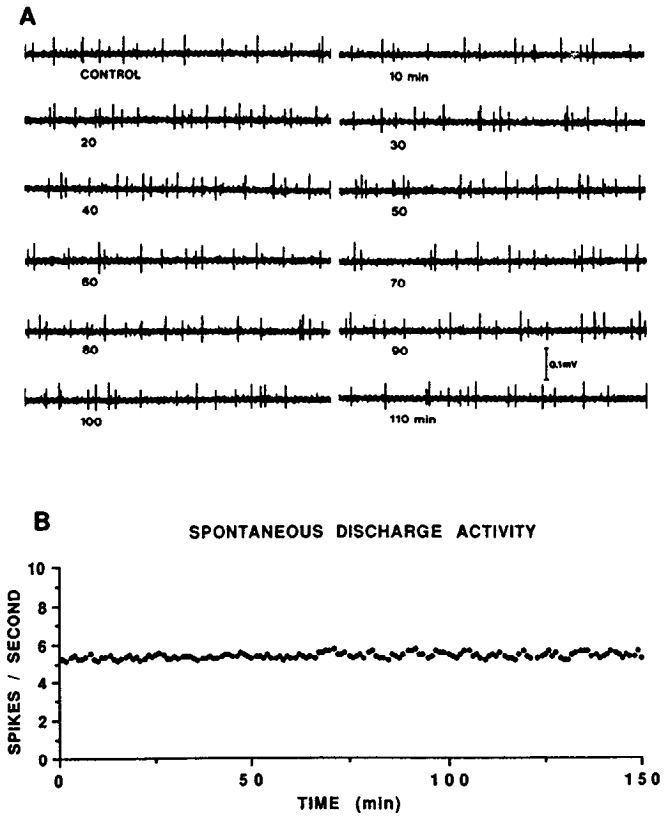

Figure 3. *A*, Recordings of spontaneous discharge activity of several (three or four) C fibers; Aδ fibers were not spontaneously active and always exhibited rapidly adapting responses to stimulation. Each sweep is 1 sec long and separated by 10 min time intervals. Note the small amplitude (<0.2 mV) of C fiber action potentials, and the stability of responses. *B*, Time versus frequency graph of the spontaneous discharge activity of a typical C fiber (large-amplitude unit in *A*), showing the small variation (5.3 ± 0.4 spikes/sec/1.0 min bin) in discharge frequency observed during a 2.5 hr continuous recording from the same nerve.

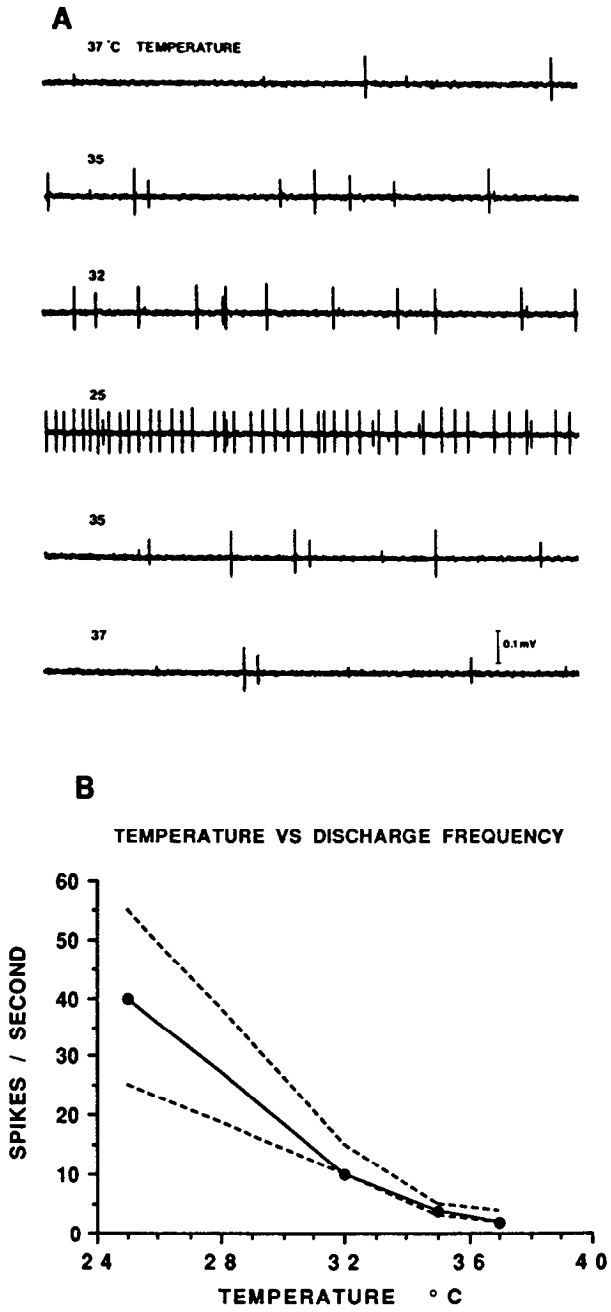

Figure 4. Thermosensitive unit discharge frequency was inversely related to temperature. *A*, One-second-long records of discharge activity at various temperatures. Discharge frequency decreased as the temperature was raised from 35°C to 37°C and increased as temperature was lowered to 25°C. *B* is a graph showing the relationship between temperature and discharge frequency of the larger-amplitude unit from *A*. *Dashed lines* indicate the range of responses recorded *in vivo*.

corneal surface. C fiber ending branches were always short (<20 μm) and appeared to wrap around and between the most superficial epithelial cells (Fig. 1*C*).

Excitability maps of Aδ and C fibers confirmed the distinct morphological differences seen with epifluorescence microscopy. C fiber endings responded to electrical stimulation in a circumscribed area in the immediate vicinity of each branching cluster, giving a punctate or spiky appearance to excitability maps (Fig. 2*A*). A given C fiber could have only a single ending in a 2 mm² test area, or as many as seven distinct endings separated by regions where discharge responses were not produced by electrical stimuli. The fiber shown in Figure 2*A* had three responsive zones separated by as little as 350 μm or by as much as 1.2 mm. Each peak in the excitability map corresponded to a cluster of nerve ending branches comparable to the one shown in Figure 1*C*, which was directly below the isolated peak in the upper right of the excitability map (Fig. 2*A*). The baseline was plotted to reflect the radius of curvature for this cornea, and the unevenness was due to spontaneous, unstimulated discharge activity observed for this fiber (compare Fig. 2*A*,*B*; the Aδ fiber was not spontaneously active). It was not possible to follow an individual C fiber between peaks because fibers traveled below the epithelium, in the subepithelial plexus, before reemerging beneath each branching cluster. Individual fibers could not be distinguished from neighboring fibers in the subepithelial plexus.

Aδ fiber excitability maps formed continuous ridges that extended over the entire length of the elongated strand endings observed with epifluorescence microscopy. Figure 2*B* shows the excitability map obtained for the Aδ fiber shown in Figure 1. Often two or three endings were observed for a given fiber in a 2 mm² test area (e.g., see Fig. 7*C*), and these appeared as parallel ridges in excitability maps. The two endings shown in Figure

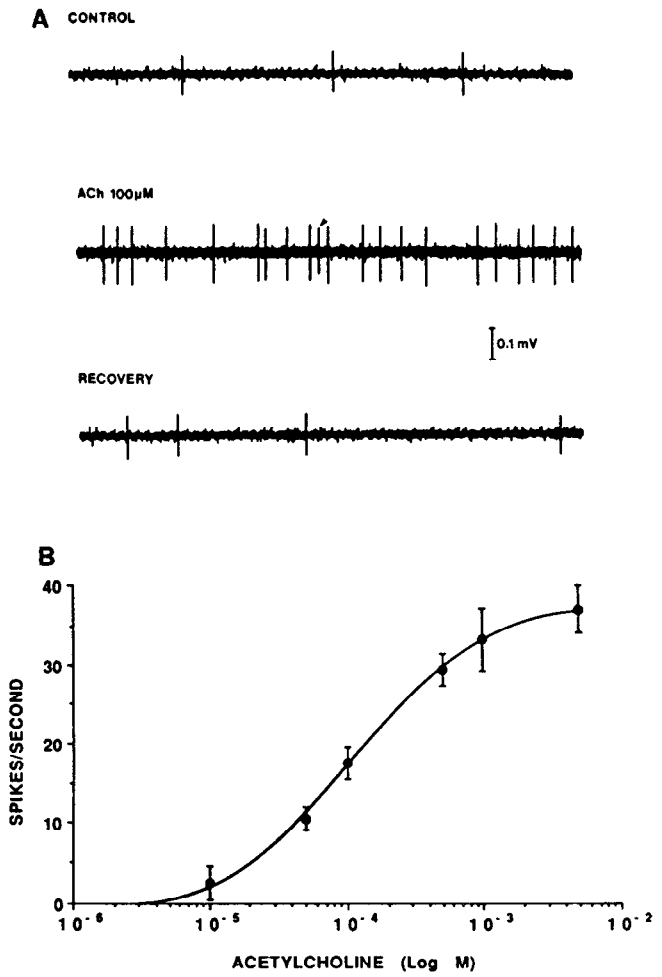

Figure 5. *A*, One-second-long records showing activation of a chemosensitive unit following application of 0.1 mM ACh to the epithelial surface. Note the decrease in spontaneous discharge of a cold-sensitive unit (*arrowhead*) following exposure to the prewarmed (37°C) ACh-containing solution. *B*, Concentration–response curve for ACh showing the minimum effective concentration of 10 μM with an EC_{50} of 100 μM. Each point represents the mean ± SD for at least four determinations at each concentration.

1*B*, however, were too closely associated (<50 μm apart) and appeared as only a single ridge in the excitability map (Fig. 2*B*).

The combined results from microscopy and excitability mapping of five Aδ fiber and eight C fiber endings are presented in a summary diagram (Fig. 2*C*). Nerve fibers running in the subepithelial plexus can branch and travel for several millimeters before forming nerve endings that migrate between epithelial cells. C fibers form endings with short branches directed in a mostly perpendicular orientation with respect to the corneal surface. Aδ fibers form endings with elongated fine strands running parallel to the corneal surface.

Spontaneous discharge activity

Multiunit recordings from corneal nerve bundles exhibited spontaneous (unstimulated) action potential activity of small amplitude (25–200 μV). Usually several (one to five) individual fibers could be discriminated on the basis of their action potential amplitude and waveform. Individual fibers (and discriminated units) exhibited tonic discharge rates of 2–7 spikes/sec [5.1 ± 0.3 (mean ± SD); $n = 42$ units] at a temperature of 35°C. Figure 3 shows a series of multiunit recordings taken at 10 min intervals from a corneal nerve bundle.

Three units were observed in these recordings based on the different action potential amplitudes exhibited. A rate meter output of the largest amplitude unit in Figure 3*A* is provided in Figure 3*B*. This unit had a discharge rate of 5.3 ± 0.1 spikes/sec with minor variance (<0.6 spikes/sec) for over 2 hr of continuous recording. Isolated corneal tissue remained viable for at least 12 hr in 16 preparations studied for this length of time. Spontaneously active units were shown to be either thermosensitive or chemosensitive afferents, but were never mechanosensitive (see below).

Thermosensitive afferents

Previous recordings from *in vivo* preparations suggested that the tonically active (spontaneous) units were thermosensitive C fibers; in particular, discharge frequency was reduced by warming the cornea and increased by cooling (Lele and Weddell, 1959; Tanelian and Beuerman, 1984). Figure 4 shows that a similar response profile was observed using the *in vitro* preparation. Warming from 35°C to 37°C resulted in a >50% decrease in firing frequency (12 spikes/sec to 5 spikes/sec; see also Fig. 9*B*). Cooling the cornea resulted in a marked increase (8–10-fold) in discharge frequency to 42 ± 4.7 (±SD; $n = 8$) spikes/sec at 25°C, for the second 1.0 sec interval following a 2.0 sec adaptation period. Effects of cooling were reversed by rewarming (Fig. 4*A*). The temperature–response graph in Figure 4*B* shows the similarity between *in vivo* (D. L. Tanelian and R. W. Beuerman, unpublished observations) and *in vitro* responses of these thermosensitive units. Conduction velocity studies using electrical stimulation of identified thermosensitive units indicated that these were unmyelinated C fibers (0.4–1.2 m/sec). Thermosensitive units were not activated by supramaximal mechanical stimulation (up to 700 dyne) or by any of the chemical agents studied (see below).

Chemosensitive afferents

A distinct population of fibers that responded to ACh and other neuroexcitatory agents was observed (Table 1, Fig. 5). Threshold for activation with ACh was 10 μM and discharge frequency increased with increasing concentrations up to 1.0 mM. Comparable excitation was produced by nicotine (1–100 μM) and carbachol (0.01–1 mM), but not by bethanecol, up to a concentration of 1.0 mM. Cholinergic-induced discharge activity was blocked by prior (5 min) and coadministration of *d*-tubocurare (0.1 mM) or κ-bungarotoxin (1.0 μM), but not by atropine (0.1 mM) or α-bungarotoxin (10 μM). Glutamate (10–100 μM) strongly activated these fibers, as did the glutamate agonist NMDA (100 μM), and both responses were enhanced in the presence of 0.1–1.0 μM glycine. The glutamate responses were blocked by the NMDA receptor antagonist APV (100 μM), MK 801 (1.0 μM), and ketamine (100 μM). Chemosensitive fibers were also activated by prostaglandin E_1 (10 μM) and by bradykinin (1.0 μM). Histamine and lactic acid did not activate these fibers at concentrations up to 1.0 mM.

Chemosensitive units had action potential amplitudes of 0.18–0.29 mV and conduction velocities of 1.1–1.8 m/sec. They were either not tonically active (9 of 14 fibers) or discharged at a low rate (0.1–2 spikes/sec), and were readily distinguished from thermosensitive units by ensuring that chemical test solutions were prewarmed to 37°C before application; thus, thermosensitive units were depressed on application of the warm test solution

Table 1. Pharmacology of agents that affected chemosensitive C fibers

Chemical	Concentration (μM)	Effect
ACh	10–1000	Strong excitation (+++)
Nicotine	1-100	Strong excitation (+++)
Carbachol	10-1000	Excitation (++)
Bethanecol	<1000	No effect
d-Tubocurare	100	Blocked cholinergic excitation
κ-Bungarotoxin	1.0	Blocked cholinergic excitation
α-Bungarotoxin	10	No effect
Atropine	100	No effect
Glutamate	10–100	Strong excitation (B) (+++)
NMDA	100	Strong excitation (+++)
Glycine	0.1–1.0	Enhanced glutamate effect
APV	100	Blocked glutamate effect
MK 801	1.0	Blocked glutamate effect
Ketamine	100	Blocked glutamate effect
Prostaglandin E_1	10	Increased discharge frequency (B) (++)
Bradykinin	1.0	Increased discharge frequency (+)

All chemicals were applied topically at 37°C to the corneal surface. Effects on fiber discharge frequency were characterized as strong (+++), medium (++), or mild (+) based on the magnitude and duration of the increased discharge activity. Some agents appeared to alter the normal single action potential discharge pattern such that burst (B) activity or grouped discharges were produced.

while chemosensitive units were activated (Fig. 5). Application of drug free solution produced only a slowing of thermosensitive unit discharge. Mechanical stimulation (up to 700 dyne) or cooling to 15°C did not activate chemosensitive afferents.

Mechanosensitive afferents

Mechanoreceptors exhibited action potential amplitudes of 0.17–0.42 mV and conduction velocities of 1.5–3.0 m/sec in the 64 units studied. They could be activated either by short-duration (2–5 msec), punctate stimuli applied perpendicular to the corneal surface (Fig. 6) or by brushing motions. Responses were rapidly adapting, and sensory thresholds of 150–250 dyne were observed for punctate stimuli. Maximal responses were observed with stimulus intensities of 220–450 dyne. Spontaneous (unstimulated) discharge activity was not recorded from any mechanosensitive fiber. These units had large receptive fields (4–6 mm^2) that were oval or wedge shaped, tapering toward the center of the cornea. It was not uncommon to find two or three mechanoreceptor afferents with overlapping receptive fields.

As pointed out above (Figs. 1, 2), Aδ mechanosensitive fibers had sensory endings made up of elongated strands with near linear trajectories traveling for distances of over 1.0 mm. Threshold for activation of these endings did not differ significantly over the length of a given ending; however, the unique elongated structure imparted directional sensitivity for mechanical stimulation (Fig. 7). Stimuli moving parallel to the long axis of these endings produced maximal activation while stimuli applied perpendicular to the long axis were least effective. The direction of movement for stimulation parallel to the long axis (i.e., distal vs proximal) did not appear to matter, except within 200 μm of the point of origin where increased sensitivity was sometimes apparent for proximally directed stimuli. Similarly,

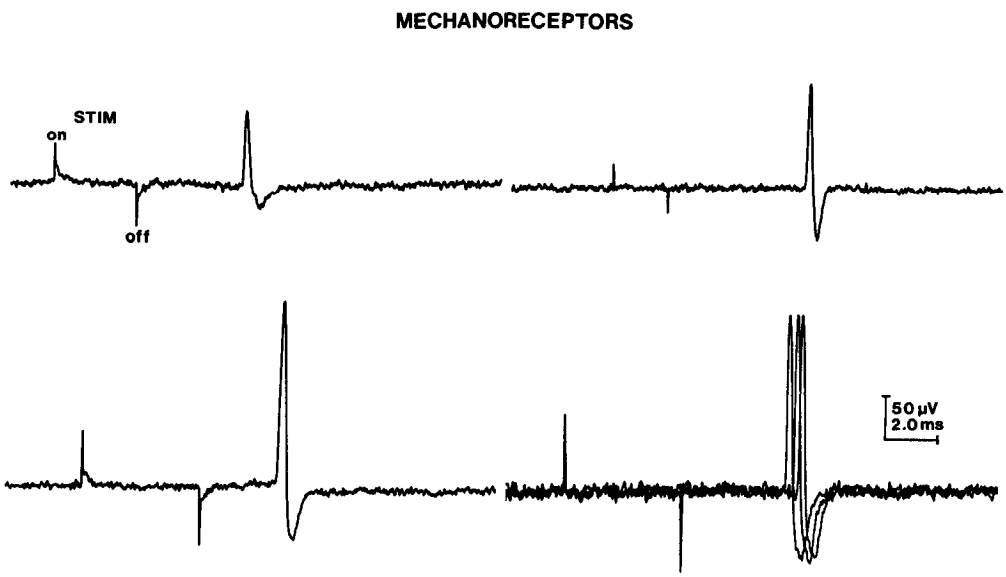

Figure 6. Example recordings of four mechanosensitive units from different preparations. A punctate mechanical stimulus (150–350 dyne; 2–5 msec) was applied at the times indicated to activate a single-unit discharge in each case. Three superimposed recordings of the same unit are provided in the *lower right* showing the latency range observed for a mechanosensitive unit stimulated at different locations (see also Fig. 8).

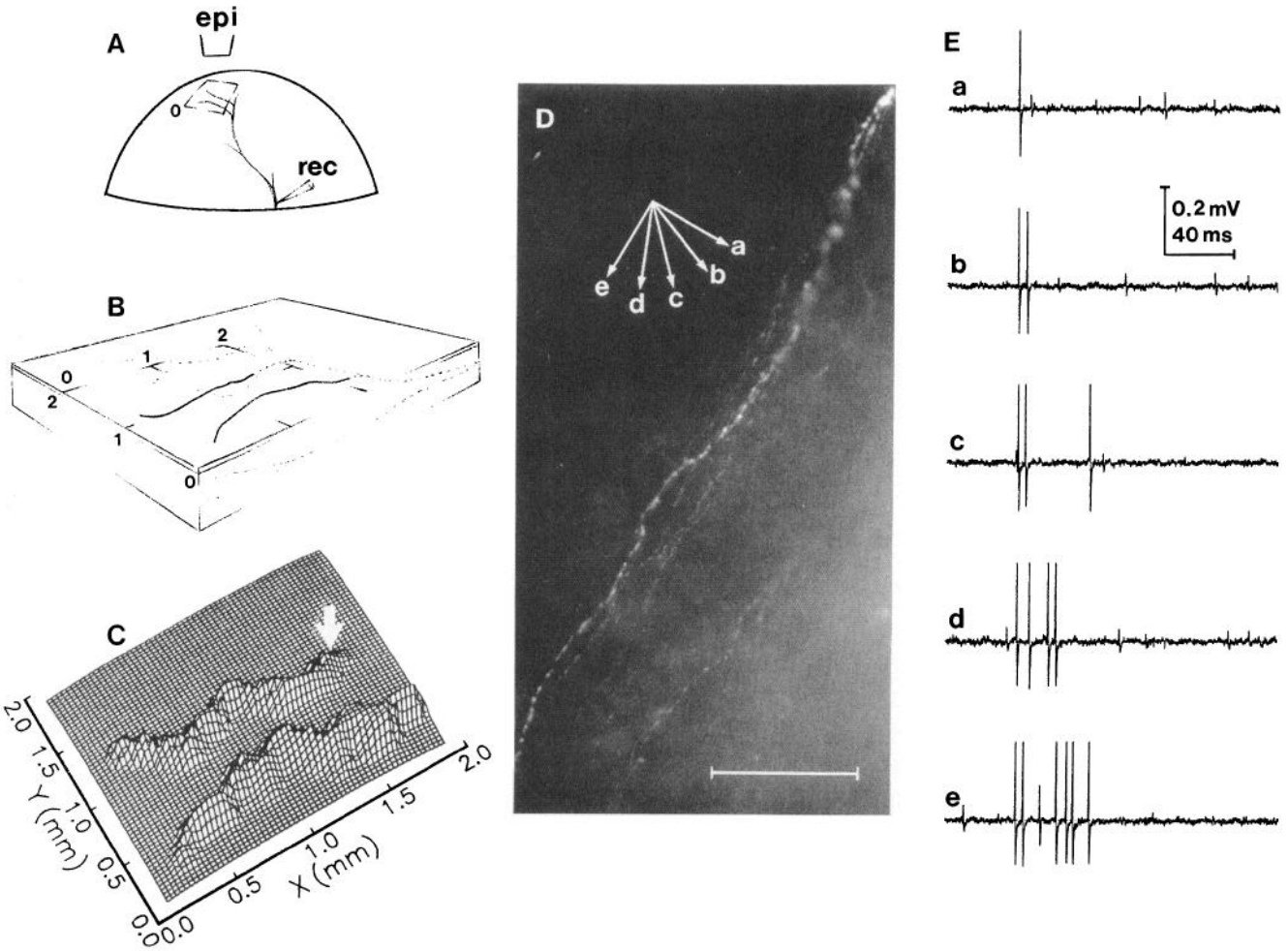

Figure 7. Mechanosensitive Aδ fibers were directionally selective. *A,* Diagram showing the receptive field, recording (*rec*) electrode placement, and epifluorescence (*epi*) microscope placement for monitoring electrical and mechanical stimuli presented to nerve endings in a 2 mm^2 area on the corneal surface. *B,* Drawing of the nerve terminal region of an Aδ fiber enlarged and transposed from *A*; the arbitrary point of origin for a 2 mm^2 area is indicated by the zero point (0, 0). The thin (40 μm) epithelial cell layer is indicated, relative to the overall thickness of the cornea (450 μm). Nerve terminals (*solid lines*) entered the epithelium from fiber branches coming off a subepithelial plexus located immediately beneath the epithelial layer, and innervated by large nerve bundles (*dashed lines*) traveling in the stroma. Excitability map (*C*) showing the stimulus:response ratio for electrical activation (10, 0.2 msec, 45 μA pulses) of the nerve endings in *A* and *B*. Discharge responses were elicited over the entire length (>1.8 mm) of each nerve ending (see also Fig. 8). *D,* Epifluorescence micrograph showing the initial segment of nerve ending indicated by the *arrow* in *C*. Direction of movement for an applied mechanical stimulus is indicated by *arrows a–e,* with respect to the long axis of this nerve ending. *E,* Action potential discharge responses following mechanical stimulation in the directions indicated in *D* (*a–e*) for this same ending. Mechanical stimulation in a direction parallel to the long axis of the nerve ending produced optimal activation; stimulation perpendicular to the ending was least effective.

responses to electrical stimulation appeared constant over the length of a given ending (Fig. 8). This constancy of responses to electrical stimulation permitted detailed studies of intraepithelial conduction velocities along the length of Aδ nerve endings. By comparing the response latencies for action potentials generated by stimuli presented at different distances along an ending, it was possible to measure conduction velocities over defined segments from distal to proximal regions of each nerve ending. Intraepithelial conduction velocities were relatively slow (0.3–1.6 m/sec) compared to the overall conduction velocity measured from the nerve ending to the recording electrode site (2.0–3.0 m/sec) for a given fiber. In addition, conduction velocities increased in a distal-to-proximal direction along each nerve ending (Fig. 8), and it was common to observe increases of two- to threefold over a distance of 1.0–2.0 mm.

Figure 9 shows the action potential discharge observed following increasing mechanical stimuli to the same region of a cornea. As stimulus intensity was increased, a low-threshold unit was activated followed by recruitment of a higher threshold afferent with a larger action potential amplitude. This high-threshold afferent exhibited the large spike amplitude (>0.3 mV) and fast conduction velocity (>3.5 m/sec) that is characteristic of "bimodal" units previously described *in vivo* (Lele and Weddell, 1959; Belmonte and Giraldez, 1981; Tanelian and Beuerman, 1984). As stimulus intensity was further increased both mechanoreceptors responded with short bursts of discharge activity (Fig. 9*A*). When threshold for mechanical stimulation was analyzed, it was apparent that two separate populations of mechanosensitive afferents were present (Fig. 9*B*). These two populations were further distinguished on the basis of modality specificity. Low-threshold mechanosensory fibers responded only to mechanical energy. Supramaximal chemical (ACh, 10 mM)

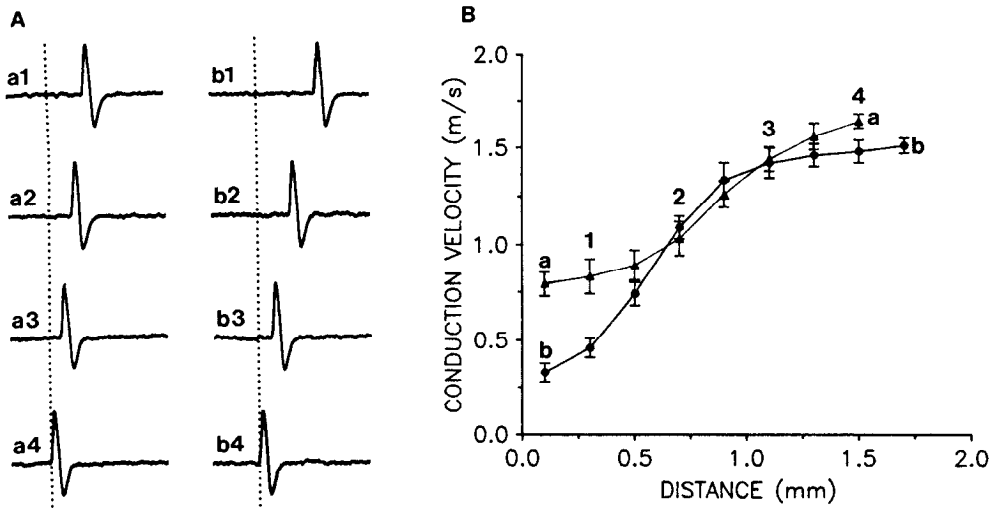

Figure 8. Mechanosensitive Aδ nerve endings were responsive to electrical stimulation for the entire length of each ending, but conduction velocity decreased toward the distal ends. *A*, Single-unit discharge recordings from the two branches (*a* and *b*) of the same Aδ fiber shown in Figure 6, responding to electrical stimulation at 400 μm intervals along the length of each nerve ending. *B*, Nerve ending conduction velocities were calculated by dividing the distance between stimulation sites by the difference in latency between action potential peak amplitudes for spike responses at 200 μm intervals. The *letters* correspond to the branches and *numbers* correspond to the stimulation sites for recordings shown in *A*. Note that nerve ending conduction velocities were considerably slower than overall fiber conduction velocity measured as the distance between stimulation and recording sites (2.65 m/sec for this same unit).

or thermal (15–50°C) stimulation did not activate low-threshold units. In contrast, high-threshold mechanosensitive units also responded to heat (see below).

Bimodal afferents

Bimodal units responded to both high-threshold mechanical (>350 dyne) and high-temperature stimuli (>40°C; Fig. 9*B,D*). A mean (±SD) spike amplitude of 0.44 ± 0.06 mV and a conduction velocity of 3.8 ± 0.2 m/sec was determined from 13 bimodal units. Sensory thresholds of 380 ± 12.5 dyne and 41.2 ± 0.8°C were determined from eight single-fiber recordings. Maximal responses were observed with mechanical stimuli of 500–600 dyne, and a temperature of 47–48°C. Mechanical stimuli of 600–700 dyne produced visible damage of the epithelium, and temperatures above 47°C changed the normally transparent epithelium to opaque. Responses from units in visibly damaged regions of epithelium were not systematically studied because sensory thresholds changed unpredictably, fibers could develop tonic (spontaneous) discharge, and the normal pattern of single spike discharge could change to high-frequency burst activity for both Aδ and C fibers. In Figure 9*C* a CO_2 laser was used to differentiate the responses of C fiber thermosensitive units and a bimodal unit following brief heat activation; the C fibers were depressed at the same time that a bimodal unit was activated by heat stimulation. Rapid adaptation to both mechanical and heat stimulation was exhibited by bimodal afferents. Bimodal units were not spontaneously active and did not respond to supramaximal chemical (ACh, 10 mM) or cold (15°C) stimuli.

Discussion

The present study characterized nerve ending morphology and electrophysiological responses of four sensory modality selective afferent fiber populations that innervate rabbit corneal epithelium. Neural activity recorded using the *in vitro* preparation can arise only from corneal receptors, since adjacent tissues (conjunctivae, iris, and lens) have been removed. Corneal nerves remained viable in isolation for at least 12 hr, and responded to stimuli known to produce sensations when applied to human cornea (Kenshalo, 1960; Schirmer, 1963; Millodot, 1973; Beuerman and Tanelian, 1979). Furthermore, action potential discharge was produced using stimulus intensities that correspond to those that produce pain, and care was taken to examine a full range of stimulus intensities, from subthreshold to supramaximal (which could produce visible damage of the epithelium). By comparing nerve ending morphology with fiber discharge activity, it was possible to demonstrate both anatomical and physiological specialization among subpopulations of corneal afferents, providing the first direct evidence to support previous suggestions of specialization in "free" nerve endings (Hensel et al., 1974; Tanelian and Beuerman, 1984; Kruger et al., 1985; Heppelman et al., 1990).

Structural differences between Aδ and C fiber free nerve endings

Electrophysiologically identified Aδ and C fibers were shown to have distinct nerve ending structures. Elongated, horizontal projections were associated with Aδ fibers and observed with both epifluorescence microscopy (Fig. 1) and in excitability mapping experiments (Figs. 2, 7). Vertically directed endings with a short branching structure were associated with C fibers (Fig. 1) and observed as punctate fields in excitability maps (Fig. 2). Structural differences among corneal nerve endings have been noted previously (e.g., Hoyes and Barber, 1976). A previous study comparing structure and function of physiologically identified Aδ mechanosensory nerve endings found "a complex of several unmyelinated axon profiles" that could "belong to (1) single fibers undulating through the plane of section, (2) a bundle of separate axons, or (3) the branching of a single axon" (Krugeret al., 1981). Although these complex axon profiles were observed in superficial epidermal layers of cat hairy skin, the multistrand nature of the terminal ending closely matches the Aδ mechanosensory endings we have observed in cornea. Similar stranded and horizontally directed processes have been observed in a number of studies of corneal (Weddell and Zander, 1950; Rozsa and Beuerman, 1982; Silverman and Kruger, 1988, 1989; Jones and Marfurt, 1991; Ogilvy et al., 1991) and other epithelium (Cauna, 1973; Novotny and Gommert-Novotny, 1988). Most corneal nerve ending studies, however, did not distinguish be-

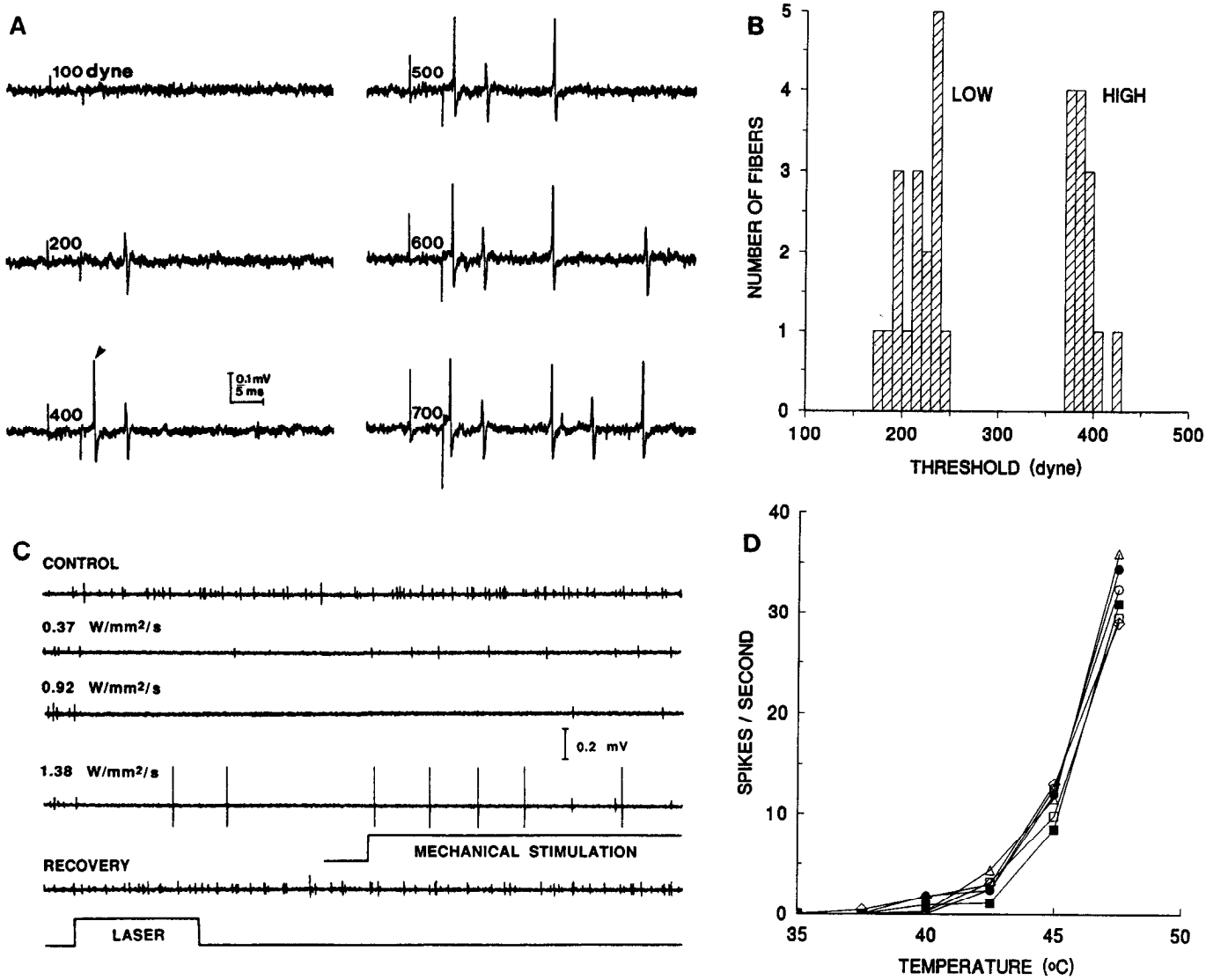

Figure 9. Recordings of mechanosensitive and bimodal units at increasing levels of mechanical and heat stimulation. In *A*, a stimulus of 4 V was sufficient to activate a small-amplitude mechanosensitive unit. As stimulus intensity increased, a larger-amplitude unit was recruited (*arrowhead*), with the high conduction velocity (>3.5 m/sec) of a bimodal type Aδ fiber. Further increases in stimulus intensity resulted in short trains of discharge from both units. (Stimulus of 1.0 V resulted in a force of approximately 50 dyne at the tip of the mechanical stimulation probe.) *B*, Histogram showing the distribution of thresholds for 30 fibers that responded to mechanical stimulation. Two populations were observed, 17 low-threshold fibers (220 ± 15 dyne, mean ± SD) and 13 high-threshold bimodal units (380 ± 12 dyne). *C*, Responses of C fibers and an Aδ bimodal unit, with overlapping receptive fields, to increasing heat stimulation from a CO_2 laser pulse. Low stimulus intensities (0.37–0.92 W/mm²/sec) reduced the thermosensitive C fiber discharge frequency. At higher stimulus intensities (1.38 W/mm²/sec) a large-amplitude bimodal unit was activated and C fiber thermal unit discharge was depressed for several hundred milliseconds. The bimodal unit's response to mechanical stimulation (520 dyne) is also shown. Complete recovery was observed within a few seconds, evidenced by the return to control discharge levels of the C fiber thermosensitive units. Each record is 1 sec long. *D*, Graph showing the instantaneous discharge frequency of several bimodal units in response to increasing temperature produced by applying 1.0 ml of preheated AQH solution to the corneal surface. Each unit was from a separate preparation, indicated by a different symbol.

tween basal epithelial axon leashes and the delicate stranded endings in superficial epithelial layers.

In contrast to the relative paucity of studies on Aδ nerve ending anatomy, there have been numerous descriptions of presumed C fiber free nerve endings that exhibit various degrees of anatomical specialization. Three distinct types of free nerve endings have been reported in human digital skin: "open endings, beaded endings and plain endings" and these exhibited "essentially vertical distribution ... in a punctate pattern" (Cauna, 1980). These punctate endings appear to be similar to the C fiber terminations we have observed in rabbit cornea, but contrast with the penicillate distribution of free endings found in human hairy skin (Cauna, 1973, 1980). As pointed out by Kruger, "free nerve endings" are rarely "free" in the strictest sense, because even the most distal processes of presumptive Aδ and C fiber sensory axons often exhibit a "focal fine structural specialization" (Kruger et al., 1985) and have been shown to be ensheathed to varying degrees by a terminal Schwann cell (Cauna, 1973; Kruger et al., 1981; Kruger, 1988). Our studies using epifluorescence microscopy lack the resolution necessary to discriminate fine structure, or even whether Schwann cell processes ensheathe nerve endings. Detailed serial reconstruc-

tions of nerve endings from identified Aδ and C fibers are required, and rabbit corneal epithelium may be an ideal tissue for studies of this nature.

Response specificity of corneal afferents

The anatomical specializations observed for free nerve endings would predict functional differences; four functionally discrete fiber populations were observed in the present study, and showed little or no overlap in sensory modality. Thermosensitive fibers did not respond to mechanical or chemical stimulation at intensities which were supramaximal for activation of other fiber types. Chemosensitive fibers were not activated by temperature changes or mechanical stimulation, and mechanoreceptors did not respond to chemical stimulation and were not activated by cooling to 15°C. Each form of stimulus consistently activated a unique population of fibers that could be reliably identified by their discharge pattern (tonic or phasic), spike amplitude, and conduction velocity (Fig. 10).

It should be noted that following visible damage to the epithelium some of the response characteristics and specificity of both Aδ and C fibers appeared to be altered. Postinjury alterations in nerve ending responses have been noted (Adriaensen et al., 1983; Belmonte et al., 1991; Handwerker et al., 1991) and are likely to play a role in hyperalgesia. The present study used low (threshold level) stimulus intensities to minimize epithelial damage. Further studies will be needed to address the response alterations observed following corneal injury.

The good correlation between spike amplitude and conduction velocity (Fig. 10) for predicting fiber type may relate to the small size of corneal nerve bundles, which places the recording electrode nearly equidistant from all fibers in the bundle. The distinction of four unique receptor populations, observed in the present study, agrees well with the distinct axon populations seen in cross-sectional spectral analysis of the rabbit ciliary (corneal) nerve (Beuerman et al., 1983), where two populations of unmyelinated fibers (median diameters of 0.52 and 1.1 μm) and two myelinated populations (2.1 and 4.0 μm) were reported. The conduction velocities of the four fiber types also distribute into four groups (Fig. 10): C fibers with median conduction velocities centered on 0.58 and 1.31 m/sec, and Aδ fibers centered on 2.35 and 3.8 m/sec. The distribution of fiber types observed in the present study (72 thermal, 64 mechanical, 14 chemical, and 13 bimodal) cannot be directly correlated to axon spectral analysis data, because physiological data were preselected by the experimental protocol (i.e., only a few fibers were recorded from each nerve in each preparation). The majority of units recorded in each nerve were thermosensitive "cold" units and low-threshold mechanosensitive fibers; bimodal and chemosensitive units were less often encountered.

Spontaneously active "cold" fibers have been observed in corneal nerve recordings from the cat (Lele and Weddell, 1959), rat (Mark and Maurice, 1977), and frog (Dawson, 1962). Dawson (1962) also noted a specific population of chemosensitive fibers that did not respond to mechanical stimulation. Lele and Weddell (1959) reported separate populations of mechanosensitive and mechano/heat (bimodal) fibers in the cat cornea. It is not known how these modality-specific responses occur in free nerve endings. An explanation for this specificity would be a selective distribution of discrete proteins (e.g., transducer/ionic channels) in each fiber type involved in the transduction of thermal, chemical, or mechanical stimulation. It is also possible that some structural differences (like those seen in the present study) could contribute to response specificity.

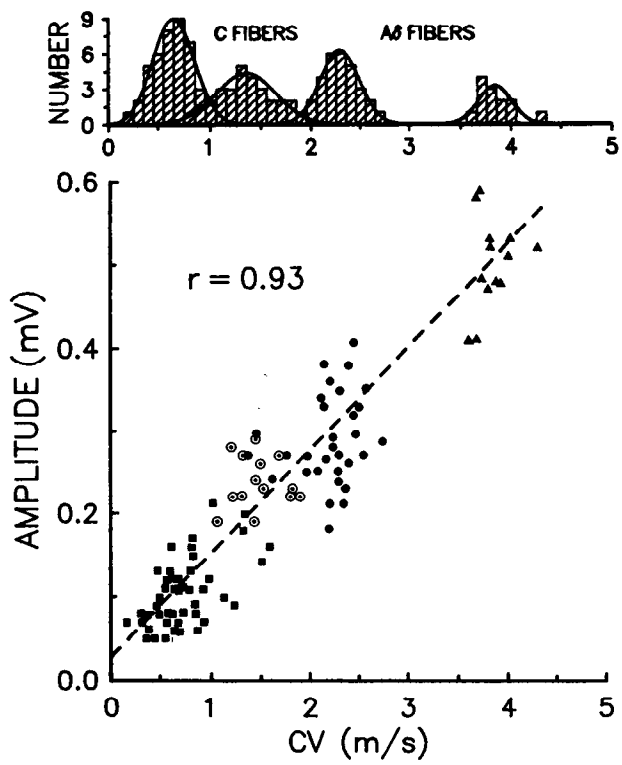

Figure 10. Graphs showing conduction velocity distribution histograms and the correlation ($r = 0.93$) between single-unit action potential amplitudes and conduction velocities, together with sensory modality for the four fiber types observed in the present study. In the *top graph,* four populations of fibers were apparent based on conduction velocity; the *solid curves* are least-squares fits to a binomial distribution. Two populations of C fibers (<2.0 m/sec) and two populations of Aδ fibers were observed. In the *bottom graph,* single-unit action potential amplitude and conduction velocity are plotted for the same data used to construct population histograms. Sensory modalities are indicated by different symbols: thermosensitive "cold" units (■), chemosensitive (⊙), low-threshold mechanosensitive (●), and bimodal mechano/heat sensitive units (▲).

Corneal afferents are similar to nociceptors in other tissues

Each fiber type, identified in the rabbit cornea, has counterparts associated with pain and nociception in other mammalian tissues, with response characteristics, conduction velocities, and sensory thresholds being similar. As pointed out by Ness and Gebhart (1990), adequate or threshold stimulus intensities for activating nociceptors can vary between tissues, and depend on the particular anatomy or geometry of nerve endings in each tissue. The nonkeratinized epithelium of cornea, for example, is relatively unprotected compared with the epithelium of skin. Free nerve endings in cornea approach to within 5 μm of the surface (Tanelian and MacIver, 1990); in contrast, there is approximately 50 μm of keratinocytes protecting free nerve endings in skin. For this reason sensory thresholds would be lower in cornea than in skin (i.e., stimulus intensities that are not noxious when applied to skin are noxious when applied to the corneal epithelium). Corneal sensory afferents satisfy the four criteria that have been proposed for nociceptors (Sherrington, 1906; Ness and Gebhart, 1990): (1) they respond to stimuli that cause tissue damage and produce pain in humans, (2) these

stimuli alter animal behavior in a way consistent with an interpretation that the stimuli are aversive, (3) the stimuli evoke basic physiological "pseudoaffective" reflexes, and (4) responses are reduced by antinociceptive manipulations that relieve pain clinically. For example, low concentrations of lidocaine (2–20 μM) block corneal injury discharge without altering nerve fiber conduction (Tanelian and MacIver, 1991), and these concentrations of lidocaine can reduce some forms of pain in humans (Tanelian and Brose, 1991).

Cold receptors from several species including the cat (Hensel et al., 1974; Duclaux et al., 1980), monkey (Dubner et al., 1975), and frog (Spray, 1974) are tonically active with discharge rates inversely proportional to temperature. Cold (temperature of <25°C) has been shown to produce the sensation of pain (Beuerman et al., 1977; Croze and Duclaux, 1978; Fruhstorfer and Lindblom, 1983) as well as stimulate cutaneous receptors in the primate (LaMotte and Thalhammer, 1982). The small action potential amplitude and slow conduction velocity recorded from these thermosensitive units are characteristic of unmyelinated C fibers.

Chemosensitive afferents were also classified as C fibers because of the slow conduction velocities (<2.0 m/sec) and tonic discharge patterns observed. Chemosensitive fiber conduction velocities overlap the range of slower conducting Aδ fibers, perhaps because conduction velocity measures for Aδ fibers were underestimated (see Materials and Methods), but are in the range of C fibers recorded in other preparations (e.g., 0.53–1.9 m/sec; Handwerker et al., 1991). The tonic discharge patterns and spontaneous activity we observed for chemosensitive and cold fibers, together with the slower conduction velocities, prompted a C fiber classification. In contrast, Aδ fibers were never spontaneously active and did not exhibit tonic discharge responses following stimulation.

Chemosensitive fibers responded vigorously to ACh, carbachol, and nicotine, and this effect was blocked by *d*-tubocurare and κ-bungarotoxin, indicating that neuronal nicotinic receptors were involved (Tanelian, 1991). In humans and animals it has been established that ACh can elicit pain: when applied to the blister base (Keele and Armstrong, 1964), intra-arterially injected (Harvey and Lilienthal, 1941; Wilson and Stoner, 1947), or instilled into the eye (Janesco et al., 1961). Given the high-concentrations of ACh present in corneal tissue, it is possible that this agent contributes to neural activation following corneal injury. In support of this, ACh causes pain when applied to the human cornea (R. W. Beuerman, personal communication; five of five subjects; M.B. MacIver and D.L. Tanelian, unpublished observations).

Corneal chemosensitive fibers also responded to prostaglandin, bradykinin, and glutamate, but were not activated by histamine or lactic acid (Table 1). The glutamate response appeared to be mediated by NMDA receptors, since it was enhanced by low concentrations of glycine (Johnson and Ascher, 1987), mimicked by NMDA, and blocked by APV, MK 801, and ketamine (Collingridge and Lester, 1989). Glutamate has been shown to activate dorsal root ganglion neurons via NMDA receptors (Lovinger and Weight, 1988), but the present study is believed to be the first to demonstrate NMDA receptors on peripheral nerve endings. The apparent insensitivity to histamine and lactic acid was surprising as these agents have been thought to play a role comparable to prostaglandins and bradykinin in signaling tissue damage to chemosensitive nociceptors (Handwerker et al., 1991; Meyer et al., 1991). The presence of chemosensitive nociceptors in human skin has been postulated (Dash and Deshpande, 1976; LaMotte, 1988), but has yet to be electrophysiologically confirmed. The chemosensitive C fiber identified in the present study is an ideal candidate for detailed studies of a purely chemosensitive nociceptor.

Aδ low-threshold mechanoreceptors identified in the present study had conduction velocities between 1.5 and 3 m/sec, which is comparable to the mean conduction velocity of 2.71 m/sec observed in the *in vivo* preparation (Tanelian and Beuerman, 1984). Thresholds for activation in both preparations were also comparable and were in the range of 150–300 dynes. These mechanoreceptors were rapidly adapting and exhibited velocity/force sensitivity (Fig. 9), a characteristic also shown for corneal mechanosensitive neurons in the trigeminal caudal nucleus (Mosso and Kruger, 1973). These receptors are well suited for detection of small moving particles, familiar irritants when trapped beneath the eyelid.

The directional sensitivity we have observed (Fig. 7) was associated with the elongated structure of these mechanosensitive nerve endings. This would be particularly important for stimuli moving across the corneal surface, but irrelevant for punctate stimuli that are the preferred form of mechanical stimulation in most previous studies of mechanoreceptors (Burgess and Perl, 1967; Belmonte et al., 1991; Handwerker et al., 1991). Directional sensitivity has also been observed for low-threshold mechanosensitive fibers innervating human tooth pulp (Trulsson et al., 1992). The slow intraepithelial conduction velocities we observed for these endings (Fig. 8) may correspond to a differential distribution of transduction proteins and/or voltage-dependent sodium channels along the length of elongated strand endings. It is possible that such a differential distribution could be present, since these endings undergo continual growth and rearrangement (Harris and Purves, 1989). The normal growth and maturation of nerve endings are in need of further study, as are the morphological and functional alterations that accompany regeneration of damaged nerves (Fried and Devor, 1988).

The bimodal population of corneal afferents are similar in response characteristics and conduction velocities to type II Aδ mechano/heat receptors (type II AMH; Campbell et al., 1979), a well-established type of nociceptor that is rapidly adapting, responsive to temperatures above 40°C, has conduction velocities of 5–25 m/sec, and is thought to be involved in transduction of pricking or first pain (Perl, 1968; Dubner et al., 1975; Georgopoulos, 1976; Fitzgerald and Lynn, 1977). Belmonte and Giraldez (1981) described a population of mechano/heat-sensitive fibers in cat cornea with similar response characteristics to the bimodal afferents observed in the present study. Smaller, spontaneously active units were also apparent (see Fig. 1*B* of Belmonte and Giraldez, 1981) and are most likely thermosensitive cold fibers; however, response characteristics of these other units were not described.

Belmonte and coworkers have recently described three subpopulations of Aδ fibers that innervate cat corneal epithelium (Belmonte et al., 1991). Two of these Aδ populations appear to be identical to the low-threshold mechanosensitive and mechano/heat fibers observed in the present study; they were not spontaneously active, were rapidly adapting, and had distinctly different mechanical thresholds. The third population responded to chemical, thermal, and mechanical stimulation, but was not observed in rabbit cornea, although we carefully searched for these fibers. It is possible that species differences exist in the distribution of both Aδ and C fiber subtypes innervating corneal

epithelium. The three Aδ fiber types were shown to have lower intracorneal conduction velocities compared to velocities measured at the limbus (Belmonte et al., 1991), consistent with the slower intraepithelial velocities seen in the present study (Fig. 8).

Corneal Aδ and C fiber relationship to sensation

Results of the present study demonstrate that corneal Aδ and C fibers can respond to selective forms of stimulation. Discrete populations of fibers were responsive to only a single form of stimulus energy (modality), except for the largest Aδ "bimodal" fibers, which responded to both high-threshold mechanical and high-temperature stimuli. The modality-specific responses apparent from electrophysiological recordings may be lost at some stage of processing in the CNS, since thermal (hot or cold) and mechanical corneal stimulations are experienced by human subjects only as irritating (for weak stimuli) or as painful (Kenshalo, 1960; Schirmer, 1963; Beuerman et al., 1977; Beuerman and Tanelian, 1979). Similarly, ACh (50 μM) produces a burning or stinging pain when applied to the cornea (R. W. Beuerman, D. L. Tanelian, and M. B. MacIver, unpublished observations). Thus, the types of corneal stimulation described in the present study produce noxious sensations. Whether these four discrete populations of modality-specific nociceptors innervate other tissues remains to be determined. At present, microneurography from human skin has identified C fiber polymodal nociceptors (Torebjork, 1974; Ochoa and Torebjork, 1989), and Aδ bimodal units (Adriaensen et al., 1983) and a host of Aδ and C fiber subtypes, with varying degrees of modality specificity, have been identified in other mammalian species (Burgess and Perl, 1967; LaMotte et al., 1983; McMahon and Koltzenburg, 1990; Handwerker et al., 1991).

It is likely that some corneal receptors serve a dual purpose, providing modality-specific information for subconscious reflex purposes and a second nociceptive function to protect the eye (especially the light path) from injury. For example, thermosensitive cold fibers may initiate the eyeblink reflex by signaling evaporative cooling (drying) of the cornea, and could also provide nociceptive input when strongly stimulated (Nagano et al., 1975; Jones and Marfurt, 1991). This would explain why the tonic activity observed in these fibers is not experienced as continuous irritation until a critical temperature (25°C), and hence discharge frequency (>40 spikes/sec), is achieved. Results of the present study, together with observations from a number of other tissues, suggest that nociception involves more than the activation of a single class of high-threshold polymodal Aδ and C fibers.

References

Adriaensen H, Gybels J, Handwerker H, Van Hees J (1983) Response properties of thin myelinated (A-delta) fibers in human skin nerves. J Neurophysiol 49:111–122.

Belmonte C, Giraldez F (1981) Response of cat corneal sensory receptors to mechanical and thermal stimulation. J Physiol (Lond) 321: 355–358.

Belmonte C, Gallar J, Pozo MA, Rebollo I (1991) Excitation by irritant chemical substances of sensory afferent units in the cat's cornea. J Physiol (Lond) 437:709–725.

Beuerman RW, Tanelian DL (1979) Corneal pain evoked by thermal stimulation. Pain 7:1–14.

Beuerman RW, Maurice DM, Tanelian DL (1977) Thermal stimulation of the cornea. In: Pain in the trigeminal region (Anderson DJ, Matthews B, eds), pp 413–422. North Holland: Elsevier.

Beuerman RW, Klyce SD, Kooner S, Tanelian DL, Rozsa A (1983) Dimensional analysis of rabbit ciliary nerve. Invest Ophthalmol Vis Sci 24:261.

Burgess PR, Perl ER (1967) Myelinated afferent fibers responding specifically to noxious stimulation of the skin. J Physiol (Lond) 190: 541–562.

Campbell JN, Meyer RA, LaMotte RH (1979) Sensitization of myelinated nociceptive afferents that innervate monkey hand. J Neurophysiol 41:1669–1697.

Cauna N (1973) The free penicillate nerve endings of human skin. J Anat 115:227–288.

Cauna N (1980) Fine morphological characteristics and micropography of free nerve endings of the human digital skin. Anat Rec 198: 643–656.

Collingridge GL, Lester AJ (1989) Excitatory amino acid receptors in the vertebrate central nervous system. Pharmacol Rev 40:143–210.

Croze S, Duclaux R (1978) Thermal pain in humans: influence of the rate of stimulation. Brain Res 157:418–421.

Dash MS, Deshpande SS (1976) Human skin nociceptors and their chemical response. Adv Pain Res Ther 1:47–51.

Dawson WW (1962) Chemical stimulation of the peripheral trigeminal nerve. Nature 196:341–345.

Dubner R, Sumino R, Wood WI (1975) A peripheral "cold" fiber population responsive to innocuous and noxious thermal stimuli applied to the monkey's face. J Neurophysiol 38:1373–1389.

Duclaux R, Schafer K, Hensel H (1980) Response of cold receptors to low skin temperatures in nose of the cat. J Neurophysiol 43:1571–1577.

Fitzgerald M, Lynn B (1977) The sensitization of high threshold mechanoreceptors with myelinated axons by repeated heating. J Physiol (Lond) 365:549.

Fried K, Devor M (1988) End-structure of afferent axons injured in the peripheral and central nervous system. Somatosens Mot Res 6:79–99.

Fruhstorfer H, Lindblom U (1983) Vascular participation in deep cold pain. Pain 17:235–241.

Georgopoulos AP (1976) Functional properties of primary afferent units probably related to pain mechanisms in primate glabrous skin. J Neurophysiol 39:71–83.

Handwerker HO, Kilo S, Reeh PW (1991) Unresponsive afferent nerve fibres in the sural nerve of the rat. J Physiol (Lond) 435:229–242.

Harris LH, Purves D (1989) Rapid remodeling of sensory endings in the corneas of living mice. J Neurosci 9:2210–2214.

Harvey AM, Lilienthal JL (1941) Observations on the nature of myasthenia gravis. Bull Johns Hopkins Hosp 69:556–577.

Hensel H, Andres K, During M (1974) Structure and function of cold receptors. Pfluegers Arch 352:1–10.

Heppelmann B, Messlinger K, Neiss WF, Schmidt RF (1990) Ultrastructural three-dimensional reconstruction of group III and group IV sensory nerve endings ("free nerve endings") in the knee joint capsule of the cat: evidence for multiple receptive sites. J Comp Neurol 292:103–116.

Hoyes AD, Barber P (1976) Ultrastructure of the corneal nerves in the rat. Cell Tissue Res 172:133–144.

Jansco N, Jansco-Gabor A, Takats I (1961) Pain and inflammation induced by nicotine, acetylcholine and structurally related compounds and their prevention by desensitizing agents. Acta Physiol 19:113–132.

Jarvis D, MacIver MB, Tanelian DL (1990) Electrophysiologic recording and thermodynamic modeling demonstrate that helium-neon laser irradiation does not affect peripheral A-delta- or C-fiber nociceptors. Pain 34:235–242.

Johnson JW, Ascher P (1987) Glycine potentiates the NMDA responses in cultured mouse brain neurons. Nature 325:529–531.

Jones MA, Marfurt CF (1991) Calcitonin gene-related peptide and corneal innervation: a developmental study in the rat. J Comp Neurol 313:132–150.

Keele CA, Armstrong D (1964) Substances producing pain and itch, pp 102–116. London: Arnold.

Kenshalo DR (1960) Comparison of thermal sensitivity of the forehead, lip, conjunctiva and cornea. J Appl Physiol 15:987–991.

Kruger L (1988) Morphological features of thin sensory afferent fibers: a new interpretation of 'nociceptor' function. Prog Brain Res 74:253–257.

Kruger L, Perl ER, Sedivel MJ (1981) Fine structure of myelinated

mechanical nociceptor endings in cat hairy skin. J Comp Neurol 198: 137–154.
Kruger L, Sampogna SL, Rodin BE, Clague J, Brecha N, Yeh Y (1985) Thin-fiber cutaneous innervation and its intraepidermal contribution studied by labeling methods and neurotoxin treatment in rats. Somatosens Res 2:335–356.
LaMantia AS, Pomeroy SL, Purves D (1992) Vital imaging of glomeruli in the mouse olfactory bulb. J Neurosci 12:976–988.
LaMotte RH (1988) Psychophysical and neurophysiological studies of chemically induced cutaneous pain and itch. In: Progress in brain research (Hamann W, Iggo A, eds), Vol 74, pp 331–335. New York: Elsevier.
LaMotte RH, Thalhammer JG (1982) Response properties of high-threshold cutaneous cold receptors in the primate. Brain Res 244: 279–287.
LaMotte RH, Thalhammer JG, Robinson CJ (1983) Peripheral neural correlates of magnitude of cutaneous pain and hyperalgesia: a comparison of neural events in monkey with sensory judgments in human. J Neurophysiol 50:1–26.
Lele PP, Weddell G (1959) Sensory nerves of the cornea and cutaneous sensibility. Exp Neurol 1:334–359.
Lovinger DM, Weight FF (1988) Glutamate induces a depolarization of adult rat dorsal root ganglion neurons that is mediated predominantly by NMDA receptors. Neurosci Lett 94:314–320.
MacIver MB, Tanelian DL (1990) Volatile anesthetics excite mammalian A-delta and C fiber nociceptor afferents recorded *in vitro*. Anesthesiology 72:1022–1030.
Mark D, Maurice D (1977) Sensory recording from the isolated cornea. Invest Ophthalmol 16:541–545.
McMahon SB, Koltzenburg M (1990) Novel classes of nociceptors: beyond Sherrington. Trends Neurosci 13:199–201.
Meyer RA, Davis KD, Cohen RH, Treede RD, Campbell JN (1991) Mechanically insensitive afferents (MIAs) in cutaneous nerves of monkey. Brain Res 561:252–261.
Millodot M (1973) Objective measurement of corneal sensitivity. Br J Ophthalmol 56:844–847.
Mosso JA, Kruger L (1973) Receptor categories represented in spinal trigeminal nucleus caudalis. J Neurophysiol 36:472–488.
Nagano S, Myers JA, Hall RD (1975) Representation of the cornea in the brainstem of the rat. Exp Neurol 49:653–670.
Ness TJ, Gebhart GF (1990) Visceral pain: a review of experimental studies. Pain 41:167–234.
Novotny GE, Gommert-Novotny E (1988) Silver impregnation of peripheral and central axons. Stain Technol 63:1–14.
(Lond) 415:583–599.
Ogilvy CS, Silverberg KR, Borges LF (1991) Sprouting of corneal sensory fibers in rats treated at birth with capsaicin. Invest Ophthalmol Vis Sci 32:112–121.
Perl ER (1968) Myelinated afferent fibers innervating the primate skin and their response to noxious stimuli. J Physiol (Lond) 197:593–615.
Rozsa AJ, Beuerman RW (1982) Density and organization of free nerve endings in the corneal epithelium of the rabbit. Pain 14:105–120.
Schirmer KE (1963) Assessment of corneal sensitivity. Br J Ophthalmol 47:488–492.
Sherrington CS (1906) The integration action of the nervous system, pp 226–230. New York: Scribner.
Silverman JD, Kruger L (1988) Lectin and neuropeptide labeling of separate populations of dorsal root ganglion neurons and associated "nociceptor" thin axons in rat testis and cornea whole-mount preparations. Somatosens Res 5:259–267.
Silverman JD, Kruger L (1989) Calcitonin-gene-related-peptide-immunoreactive innervation of the rat head with emphasis on specialized sensory structures. J Comp Neurol 280:303–330.
Spray DC (1974) Characteristics, specificity and efferent control of frog cutaneous cold receptor. J Physiol (Lond) 237:15–38.
Tanelian DL (1991) Cholinergic activation of a population of corneal afferent nerves. Exp Brain Res 86:414–420.
Tanelian DL, Beuerman RW (1984) Responses of rabbit corneal nociceptors to mechanical and thermal stimulation. Exp Neurol 84:165–178.
Tanelian DL, Brose WG (1991) Neuropathic pain can be relieved by drugs that are use-dependent sodium channel blockers: lidocaine, carbamazepine, and mexiletine. Anesthesiology 74:949–951.
Tanelian DL, MacIver MB (1990) Simultaneous visualization and electrophysiology of corneal A-delta and C fiber afferents. J Neurosci Methods 32:213–222.
Tanelian DL, MacIver MB (1991) Analgesic concentrations of lidocaine suppress tonic A-delta and C fiber discharges produced by acute injury. Anesthesiology 74:934–936.
Torebjork HE (1974) Afferent C units responding to mechanical, thermal and chemical stimuli in human non-glaborens skin. Acta Physiol Scand 92:374–390.
Tower SS (1940) Unit for sensory reception in cornea. J Neurophysiol 3:486–500.
Trulsson M, Johansson RS, Olsson KA (1992) Directional sensitivity of human periodontal mechanoreceptive afferents to forces applied to the teeth. J Physiol (Lond) 447:373–389.
Weddell G, Zander E (1950) A critical evaluation of methods used to demonstrate tissue neural elements, illustrated by reference to the cornea. J Anat 84:168–195.
Wilson A, Stoner HB (1947) The effect of the injection of acetylcholine into the brachial artery of normal subjects and patients with myasthenia gravis. Q J Med 16:237–243.
Zander E, Weddell G (1951) Observations on the innervation of the cornea. J Anat (Lond) 85:68–99.